

Equilibrium, Thermodynamic and Kinetic Studies on Adsorption of Zinc (II) From Solutions Using Different Low-Cost Adsorbents

Pascal C. Njoku¹, Atu A. Ayuk¹, Atulegwu P. Uzoije², Justus I. Okolie¹

¹Department of Chemistry, Federal University of Technology, Owerri, Imo State, Nigeria

²Department of Environmental Technology, Federal University of Technology, Owerri, Imo State, Nigeria

Email Address

justusokolie@yahoo.com (J. I. Okolie), emynjoku2006@yahoo.com (P. C. Njoku)

To cite this article

Pascal C. Njoku, Atu A. Ayuk, Atulegwu P. Uzoije, Justus I. Okolie. Equilibrium, Thermodynamic and Kinetic Studies on Adsorption of Zinc (II) From Solutions Using Different Low-Cost Adsorbents. *American Journal of Chemistry and Applications*. Vol. 2, No. 6, 2015, pp. 129-140.

Abstract

Many industrial wastewaters contain numerous toxic metals such as zinc, which must be removed before reuse of the water or discharge into the environment. In this present study, unripe plantain peel activated carbon (UPPAC), pineapple peel activated carbon (PPAC) and commercial activated carbon (CAC) were utilized as low cost adsorbents for the removal of Zn (II) from aqueous solutions. Batch adsorption methodology was used to evaluate the effect of solution pH, initial metal ion concentration, adsorbent dose, contact time and temperature on adsorption. Scanning Electron Microscope (SEM) and Fourier Transform Infrared Spectrophotometer (FTIR) were used to characterize the adsorbents. The equilibrium isotherm data were analyzed using the Langmuir, Freundlich and Temkin isotherm model. The kinetic data were analyzed using the pseudo-first order, pseudo-second order equations, Elovich equation and intraparticle rate equation. Maximum adsorption of Zn (II) on UPPAC, PPAC and CAC (82.45%, 89.95% and 93.45%) was observed at pH 6 and pH 7. The adsorbed amount of Zn (II) increased with increase in contact time and reached equilibrium within 180 minutes. The maximum adsorption was found to be 200 mg/L in the studied range (200 – 1000 mg/L). The adsorption capacity and percent removal of Zn (II) were found to increase with increase in temperature. The Freundlich isotherm models provided the best fit to the experimental data for Zn (II) as indicated by the regression coefficient values ($R^2 > 0.97$). The pseudo-second order equation gave the best fit to the experimental data for the metal ion ($R^2 > 0.99$). Thermodynamic analysis showed a spontaneous adsorption process as negative values of ΔG^0 (-1.269 to -5.530) were obtained at all temperatures. The positive enthalpy change ΔH^0 , 18.00, 20.46 and 23.45 kJ mol⁻¹ for UPPAC, PPAC and CAC indicated an endothermic process. A highly disordered process was indicated by the positive entropy change ΔS^0 .

Keywords

Activated Carbon, Zn (II), Adsorption, Heavy Metals, Adsorption Kinetics, Adsorption Isotherms

1. Introduction

Among all the possible pollutants that are responsible for the contamination of surface and ground water, heavy metals are most important. They pose great risks to humans, plants and animals because of their extremely toxic effects and have been the main reason behind large number of afflictions [1]. These contaminated aqueous waste streams with heavy metals generated from the industries are the main source of polluting ground water and other resources of water. Heavy metals tend to accumulate in the living organisms since they are not

readily biodegradable and cause various diseases and disorders [2].

The discharge of wastewaters containing heavy metals to the environment have increased tremendously in developing countries as a result of growth of industries such as metal plating facilities, mining operations, fertilizer industries, tanneries, batteries, paper industries and pesticides, etc. [3]. Through food chain these heavy metals reach human body.

Zinc is present in the air, soil, water and almost all foods.

Zinc is naturally released into the environment, although industrial activities are mostly responsible for zinc pollution. Mining and foundry activities, zinc, lead and cadmium refining, steel production, carbon combustion and solid waste incineration all lead to the release of zinc into the environment [4]. Water reservoirs are contaminated by the run-off from these industries. Zinc is commonly used to coat iron and other metals for prevention of oxidation. Various zinc salts are used industrially in wood preservatives, catalysts, photographic paper, accelerators for rubber vulcanization, ceramics, textiles, fertilizers, pigments and batteries [4].

Zinc is an essential element in bio-molecules and its uptake by living organisms is important. However, excessive concentrations of zinc from metal refining and manufacturing processes wastewaters result in damages to human health causing disruptions in metabolism and arteriosclerosis [5]. Zinc exposure causes depression, lethargy, neurological signs and increase in thirst [6].

Several processes are currently used in industry for the removal of heavy metals from aqueous solutions. Ion exchange, adsorption, reverse osmosis, chemical precipitation and sedimentation, filtration, electrodialysis and air flotation are among those methods most commonly employed [7].

Investigation into new and cheap methods of metal ions removal from industrial wastewater is gaining continuous research attention, with adsorption process suggested as most economically viable method. Thus, this study intends to use adsorption process for heavy metals removal from industrial effluents because it has been reported to be inexpensive, widely applicable, efficient, and creates relatively little sludge [8].

One of the major methods for the removal of pollutants from aqueous effluent is adsorption by using porous solid adsorbents. Adsorption has demonstrated its efficiency, easy handling, availability of different adsorbents, and economic feasibility as a wastewater treatment process compared to the other purification and separation methods, and has gained importance in industrial applications [9]. Biosorption is the natural capability of the biomass to immobilize dissolved components, e.g. heavy metal ions, on its surface. Recent studies showed that common agricultural waste products or natural polymers can be used as potential biosorbents for the removal of heavy metals [10]. Biosorption can be used for the treatment of wastewater with low heavy metal concentration as an inexpensive, simple and effective alternative to conventional methods.

In the present work the sorption of zinc ions from aqueous solution by using unripe plantain peel activated carbon (UPPAC), pineapple peel activated carbon (PPAC) which are readily available materials and commercially activated carbon (CAC) were investigated. The effects of adsorbent dosage, contact time, temperature, initial metal ions concentration and pH on the removal of zinc ions were investigated and the experimental data obtained were evaluated and fitted using adsorption equilibrium isotherms models, kinetic models and thermodynamic studies.

2. Materials and Method

2.1. Materials

All reagents used in this study were of analytical grade. The carbonaceous precursors that were used for the preparation of activated carbon are pineapple peel and unripe plantain peel. Zinc nitrate ($\text{Zn}(\text{NO}_3)_2 \cdot 6\text{H}_2\text{O}$) was used for the preparation of zinc stock solution. Commercial activated carbon, cylinders, volumetric flasks, beaker, conical flasks, sample bottles, phosphoric acid, nitric acid, sodium hydroxide, distilled water, muffle furnace (Vecstar limited England), crucibles, funnels, filter papers, sieves, Electronic weighing balance Citizen model CY, water bath model TT60D multi-purpose Techmel USA, scanning electron micrograph (Phenom ProX SEM machine), Fourier transform infrared spectrophotometer (SHIMADZU FTIR-8400S), oven, centrifuge (Unico power spin Mx), atomic absorption spectrophotometer (UNICAM SOLAR 969 AAS).

2.2. Preparation of Unripe Plantain Peels and Pineapple Peels Adsorbents

Unripe plantain peels and pineapple peels were collected from fruit sellers in the streets of Owerri. The plantain peels and pineapple peels were washed first with tap water to remove dirt and mud and finally washed with distilled water. After washing, they were sun-dried for about two weeks, before grinding with a roller mill. The ground plantain peels and pineapple peels were sieved with a sieve of mesh sizes 1.00 mm – 1.18 mm. The precursor obtained was washed with distilled water to remove surface bound impurities and dried in the oven at 100°C for 24 hours. 200 g of each sample was mixed with 400 ml of 1 M H_3PO_4 until the mixture formed a paste. The paste was dried in the oven at 100°C for 24 hours. After drying in the oven, the sample was transferred to a crucible and pyrolysed in a muffle furnace at 300°C for 2 hours. The pyrolysed material was finally washed with distilled water to bring its pH to 7 and oven dried for 24°C hours to get a plantain peel and pineapple peel based carbon

2.3. Determination of Surface Chemistry

The surface functional groups of the activated carbon were estimated by Fourier Transform Infra-red Spectrophotometer (FTIR). FTIR of the different samples was recorded within 500 cm^{-1} - 4500 cm^{-1} . Samples of 0.1 g was mixed with 1 g of KBr, spectroscopy grade (Merk, Darmstadt, Germany), in a mortar. Part of this mix was introduced in a cell connected to a piston of a hydraulic pump giving a compression pressure of 15 kPa / cm^2 . The mixture was converted to a solid disc which was placed in an oven at 105°C for 4 hours to prevent any interference with any existing water vapor or carbon dioxide molecules from the atmosphere. It was then transferred to the FTIR analyzer and a corresponding chromatogram was obtained showing the wave lengths of the different functional groups in the sample.

2.4. Scanning Electron Microscopy

The surface morphology of the activated carbon samples were analyzed by Scanning Electron Microscope (SEM). Surface topographical information was obtained by a surface morphological study in Phenom Prox Scanning Electron Microscope. Well ground carbon samples were placed on a sample stub with the aid of a graphite conductive adhesive paste before being firmly loaded on a cylindrical rod which serves as the sample holder. The rod was thereafter placed in the analysis chamber of the SEM which remains under vacuum all through the analysis. When excited primary beam of electrons from the light source strikes a sample, various secondary electrons from the sample surface were emitted which are characteristic of each of the samples. Various secondary electron detectors attract the scattered electrons, and the signals were read.

2.5. Preparation of Zinc Stock Solution

All the reagents used in this study were of analytical grade, obtained from Sigma–Aldrich and used without further purification. The working zinc solutions were prepared by measuring 4.55 g of zinc nitrate Zn(NO₃)₂ · 6H₂O using a weighing balance and dissolving in 1000 ml distilled water. After dissolving, the mixture was stirred properly on a magnetic stirrer for proper mixing. The working solutions were prepared by dilution of the stock solution with double distilled water to obtain solution of concentration 200 to 1000 mg/L.

2.6. Adsorption Experiments

The adsorption was carried out in 60 ml pretreated plastic bottles with an adsorbent dose of 0.1 g, metal concentration of 200 mg/L, pH at 6, 180 min contact time and temperature of 28°C. This was done by contacting 0.1 g of UPPAC, PPAC and CAC separately with 50 ml of metal solution. The effect of initial metal ion concentration was carried out by varying Zn (II) ion concentration from 200-1000 mg/L. The effect of pH was carried out at pH values from 2-8. The effect of adsorbent dose was determined by varying doses from 0.1-0.5 g. The effect of contact time was conducted by varying the contact time from 10-180 min. The effect of temperature was investigated by varying the adsorption temperature from 28°C -70°C. The filtrate was centrifuged before it was analyzed using AAS. All the experiments were done in triplicate and the mean values were used.

The amount of metal adsorbed q_e (mg/g) was determined using equation (1):

$$q_e = \frac{(C_o - C_e)V}{m} \dots\dots\dots(1)$$

where m is the mass of adsorbent (g), V is the volume of solution (L), C_o is the initial concentration of metal (mg/L), C_e is the equilibrium metal ion concentration (mg/L) and q_e is the amount of metal adsorbed at equilibrium (mg/g).

The percent removal of metals from the solution was calculated using equation (2):

$$\% R = \frac{C_o - C_e}{C_o} \times 100 \dots\dots\dots(2)$$

where C_o is the initial metal ion concentration in (mg/L) and C_e is the final metal ion concentration which is also the equilibrium metal ion concentration of solution in (mg/L).

2.7. Adsorption Isotherm

The Langmuir, Freundlich and Temkin isotherms are the most frequently used models to describe the experimental data of adsorption. In the present work these three isotherms were applied to investigate the adsorption process of Zn (II) on UPPAC, PPAC and CAC at different conditions of operating parameters. The adsorption equilibrium study was carried out for metal concentrations varying from 200 to 1000 mg/l. The applicability of the isotherm equation to the adsorption study done was compared by judging the correlation coefficients R^2 .

2.8. Kinetic Analysis

The kinetics of the adsorption of an adsorbate on an adsorbent governs the rate, which determines the residence time and helps in defining the efficiency of an adsorbent. This can be controlled by several independent processes which could act in series or parallel such as bulk diffusion, chemisorptions, intraparticle diffusion, physisorption and mass transfer. In order to investigate the kinetics of sorption, four models were applied in this study which includes the pseudo-first order, pseudo-second order, intraparticle diffusion model and Elovich model. These models were assessed based on their regression parameters R^2 to indicate if applicable or not to the adsorption process.

2.9. Thermodynamics Study

The nature of the adsorption of adsorbate on the adsorbent is predicted by estimating the thermodynamic parameters. The changes in thermodynamic parameters such as free energy ΔG° , enthalpy change ΔH° and entropy change ΔS° were determined to evaluate the feasibility of the adsorption process. The standard free energy of the adsorption is related to the thermodynamic equilibrium constant (K_C) by the following equation [11, 12].

$$\Delta G^\circ = -RT \ln K_C \dots\dots\dots(3)$$

where T is the temperature (K), R is the ideal gas constant (8.314 J/molK) and K_C is defined by the equation

$$K_C = \frac{C_a}{C_e} \dots\dots\dots(4)$$

where C_a (mg/L) and C_e (mg/L) are the equilibrium concentration for solute on the adsorbent and in solution respectively. Also, the Gibbs free energy is related to the enthalpy change (ΔH°) and entropy change (ΔS°) at a constant temperature by the Van't Hoff equation, equation (5) [13].

$$\ln K_C = -\frac{\Delta G^\circ}{RT} = -\frac{\Delta H^\circ}{RT} + \frac{\Delta S^\circ}{R} \dots\dots\dots(5)$$

The values of ΔH° and ΔS° are calculated from the slope and intercept of the plot ($\ln K_C$ versus $1/T$).

3. Results and Discussion

3.1. FTIR Studies

(Figs 1-3) show FTIR spectra for the adsorbents. Variations of bands were observed on the adsorbents used for this study. The sharp bands occurring at 3996.64 cm^{-1} - 3454.62 cm^{-1} are due to the presence of both free and hydrogen bonded $-\text{OH}$ group on the adsorbent surface. The bands at 2900 cm^{-1} , 2947.33 cm^{-1} and 2934.79 cm^{-1} can be attributed to C-H stretching of alkanes. The peaks at 1725.38 cm^{-1} , 1746.60 and 1704.17 cm^{-1} are due to C=O stretch in normal aliphatic

ketones, ester and carboxylic acid. The bands occurring at 1555.64 cm^{-1} - 1470.77 cm^{-1} may be attributed to N-H bend in primary and secondary amines and N=O asymmetric string stretch and C=C vibration. The bands appearing at 1442 cm^{-1} - 1048 cm^{-1} are due to CH_2 characteristics bending and S=O in sulphoxides. The strong band occurring at 642.32 cm^{-1} and 585.42 cm^{-1} are attributed to the presence of C-Br stretch in aliphatic bromide. The band occurring at 497.65 cm^{-1} - 421.46 cm^{-1} are due to the presence of C-I stretch in aliphatic iodide. The FTIR of the adsorbents indicate that the hydroxyl and carboxyl groups are in abundance in CAC followed by PPAC and UPPAC. CAC and PPAC showed high adsorption capacity for Zn (II) when compared with UPPAC.

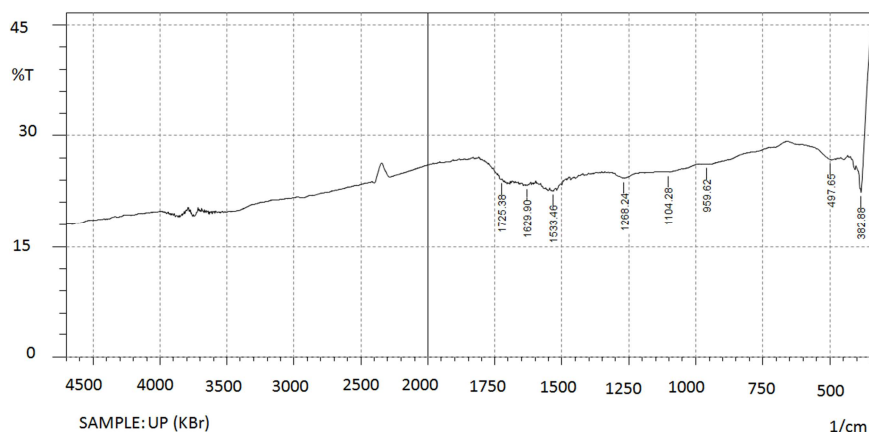


Fig. 1. FTIR spectrum UPPAC.

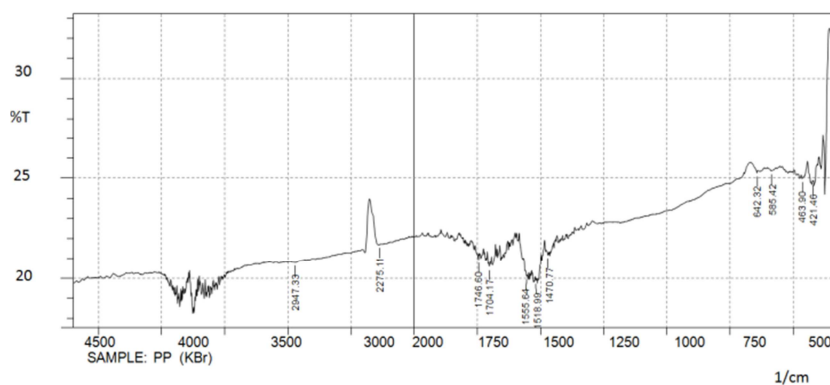


Fig. 2. FTIR spectrum of PPAC.

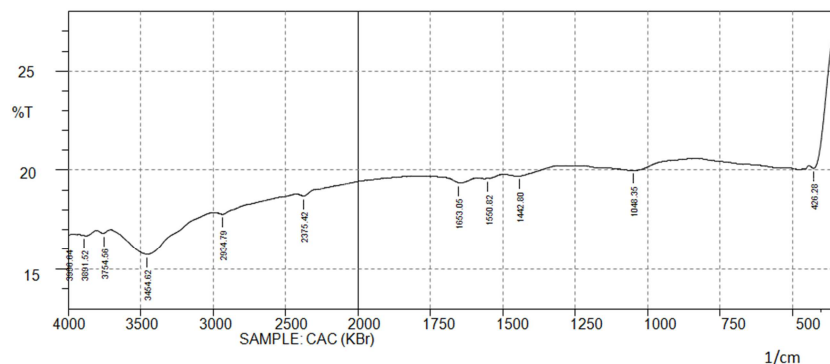


Fig. 3. FTIR spectrum of CAC.

3.2. Scanning Electron Microscopy

Physical morphology study of the adsorbent surfaces showed texture with heterogeneous surfaces and variety of pore sizes and cavities as shown in figures (4-6). Pores and cavities are responsible for increase in surface area, adsorption capacities and efficiencies [14, 15]. It was observed that CAC and PPAC have higher number of pores and cavities than UPPAC. Consequently, Zn (II) adsorption on various adsorbents (CAC, PPAC and UPPAC) varies accordingly. Adsorption was higher in CAC and PPAC apparently due to high surface area and pore sizes.

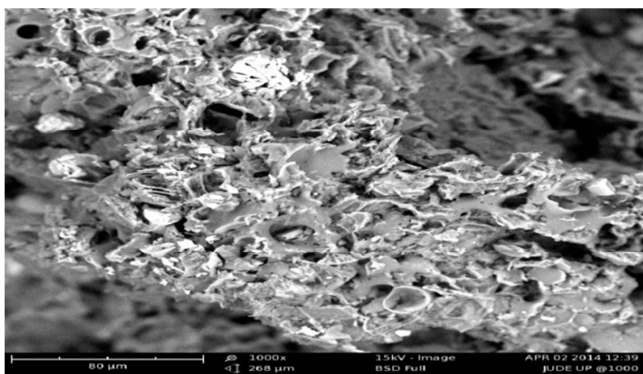


Fig. 4. SEM image of UPPAC at 1000x.

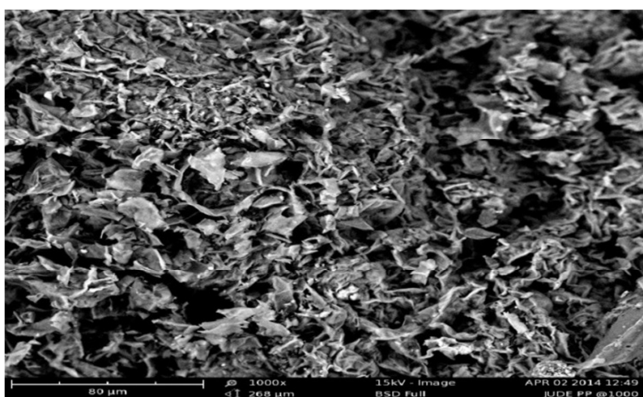


Fig. 5. SEM image of PPAC at 1000x.

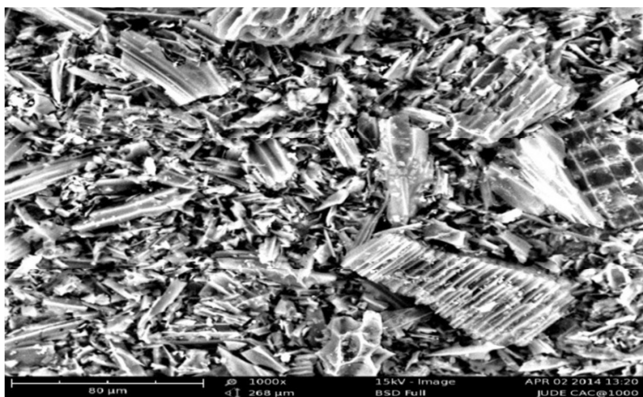


Fig. 6. SEM image of CAC at 1000x.

3.3. Effect of pH

pH is one of the most important parameters controlling uptake of heavy metals from wastewater and aqueous solution. (Figure 7) shows the effect of pH on Zn²⁺ removal by UPPAC, PPAC and CAC. These studies were conducted at a constant initial metal ion concentration of 200 mg/L, adsorbent dose of 0.1 g/L, contact time of 180 minutes and at room temperature.

The maximum removal for Zn²⁺ was found to be 82.45 % by UPPAC at pH 6, 88.95 % by PPAC at pH 6 and 93.45 % by CAC at pH 7. The maximum adsorption at pH 6 may be attributed to the partial hydrolysis of M⁺ resulting in the formation of MOH⁺ and M(OH)₂. M(OH)₂ would be adsorbed to a greater extent on the non-polar adsorbent surface, compared to M²⁺. With increase in pH from 2 to 6 the metal exists as M(OH) in the medium and surface protonation of adsorbent is minimum, leading to the enhancement of metal adsorption. At higher pH, that is above optimum pH of 6, increase in OH⁻ ions cause a decrease in adsorption of metal ions at adsorbent-adsorbate interface [16].

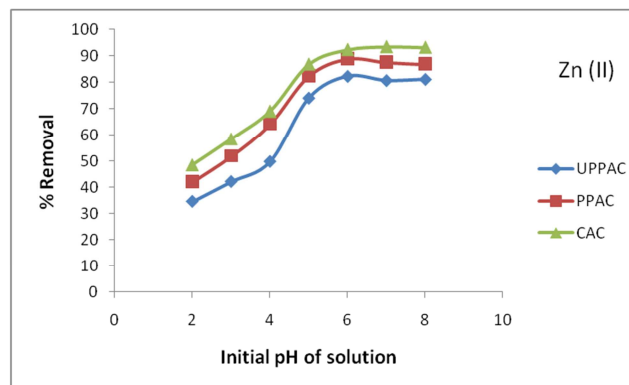


Fig. 7. Effect of pH on percentage removal of Zn (II). Initial metal ion concentration 200 mg/L, 0.1 g adsorbent dose, 180 min contact time and 28°C temperature.

3.4. Effect of Adsorbent Dose

The effect of adsorbent dose on the adsorption of Zn (II) ion using UPPAC, PPAC and CAC was illustrated in (figures 8). Different doses of adsorbents ranging from 0.1-0.5 g/L were considered and other operating parameters were maintained (metal concentration-400 mg/L, contact time-180 min, pH 6.0 and temperature 28°C). From the experiment, it was observed that percent adsorption increased with increase in adsorbent dose. The maximum percent removal by UPPAC was 85.93, 87.7 by PPAC and 89.8 by CAC. CAC had a better adsorption than PPAC and UPPAC. It is apparent that the percent removal of heavy metals increases rapidly with increase in the dose of adsorbents due to the greater availability of the exchangeable sites or surface area. Moreover the percentage of metal ion adsorption on adsorbent is determined by the adsorption capacity of the adsorbent for various metal ions [17].

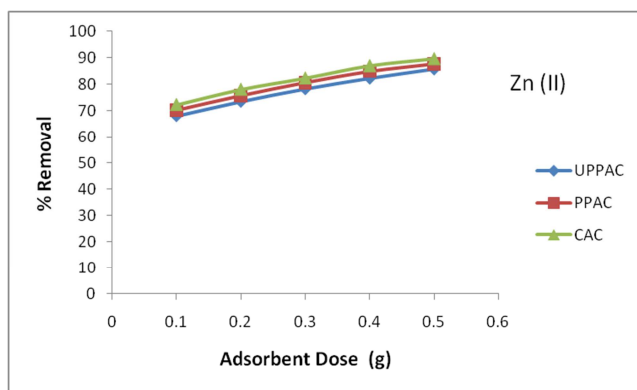


Fig. 8. Effect of adsorbent dose on percentage removal of Zn (II). Initial metal ion concentration 400 mg/L, pH 6, 180 min contact time and 28 °C temperature.

3.5. Effect of Metal Ion Concentration

The effect of Zn (II) ion concentration on UPPAC, PPAC and CAC was studied. Various concentration of Zn (II) ion solution of 200 mg/L, 400 mg/L, 600 mg/L, 800 mg/L and 1000 mg/L were used to study their effect on the percent removal and adsorption capacity of Zn (II) ions, keeping the other parameters constant at pH 6, 180 minutes contact time, room temperature and 0.1 g adsorbent dose. Figure 9 shows the percent of Zn (II) removal by UPPAC, PPAC, and CAC. From figures 9, it can be seen that percent removal of Zn (II) decreases with increase in initial heavy metal concentration. For Zn (II) ion, the maximum percent removal by UPPAC is 82.45%, 88.95% by PPAC and 92.35 % by CAC.

At lower initial metal ion concentrations, sufficient adsorption site are available for adsorption of the heavy metal ions. However at higher concentrations, the numbers of heavy metal ions are relatively higher compared to availability of adsorption site [18]. Hence, the percent removal of heavy metals depends on the initial metal ion concentration and decreases with increase in initial metal ion concentration.

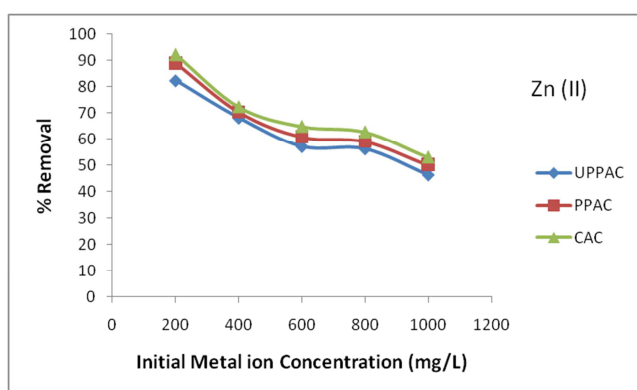


Fig. 9. Effect of initial metal ion concentration on percentage removal of Zn (II). 0.1 g adsorbent dose, pH 6, 180 minutes contact time and 28°C temperature.

3.6. Effect of Contact Time

The effect of contact time on the percent removal of Zn (II) ion on UPPAC, PPAC and CAC was studied. These studies

were conducted at constant initial metal ion concentration of 200 mg/L, adsorbent dose of 0.1 g/L, pH at 6.0 and at 28°C. From (figure 10), it was observed that the rate of removal of the adsorbate increased with time, until an equilibrium time was achieved. Equilibrium time was achieved at about 90 minutes, and increased slightly upto 180 minutes. Hence, a contact time of 180 minutes was chosen to ensure optimum removal of metal ions. CAC had a better adsorption than PPAC and UPPAC. CAC had the highest adsorption of 92.35% at 180 minutes, 88.95% by PPAC and 82.45% by UPPAC at 180 minutes respectively. The adsorption was noticed to be fast initially and then became slower which can be attributed to the strong attractive force between the ions and the adsorbent [19].

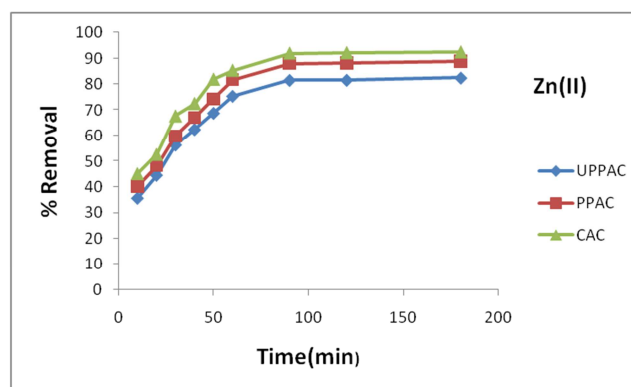


Fig. 10. Effect of contact time on percentage removal of Zn (II). 0.1 g adsorbent dose, pH 6, 200 mg/L initial metal ion concentration and 28°C temperature.

3.7. Effect of Temperature

Effect of temperature on Zn (II) adsorption on UPPAC, PPAC and CAC is shown in figure 11. Experiments were performed in the temperature range 28 to 70°C at constant Zn (II) concentration (400 mg/L), adsorbent dose (0.1 g), contact time (180 minutes) and pH 6 for UPPAC, PPAC and CAC. Adsorption of Zn (II) on all adsorbents witnessed the increase in percent removal (% R) and adsorption capacity (q_e). The percent removal of Zn (II) on UPPAC, PPAC and CAC increased from 62 to 79.93, 66.23 to 83.68 and 68.58 to 87.43% with rise in temperature from 28 – 70°C. The increase in percent removal of Zn (II) with increase in temperature by the adsorbents indicates an endothermic process. At higher temperatures, the rate of diffusion of solute within the pores of the adsorbent increases since diffusion is an endothermic process. Thus, the percent removal of Zn (II) increases as the rate of diffusion of the ions in the external mass transport process increases with temperature [20]. The high percent removal of Zn (II) in case of CAC may be due to the high diffusion rate of Zn (II) ions onto the pores as a result of larger surface area and pore volume of the adsorbent when compared to the other two types. Moreover, at low temperature, the kinetic energy of Zn (II) is low and hence contact between the metal ions and active sites of the adsorbent are insufficient, resulting in reduced adsorption efficiency.

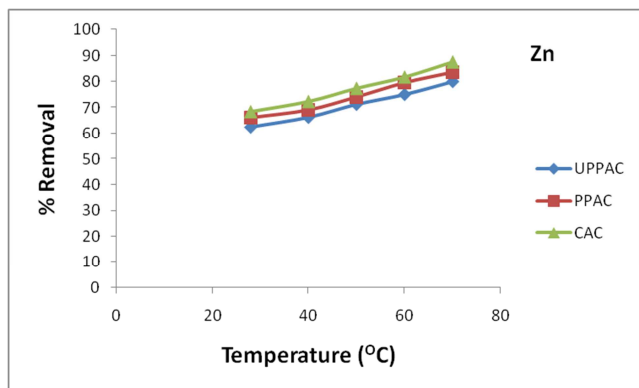


Fig. 11. Effect of temperature on percentage removal of Zn (II). 0.1 g adsorbent dose, pH 6, 180 minutes contact time and 400 mg/L initial metal ion concentration.

3.8. Adsorption Isotherm

Adsorption isotherm expresses the relationship between the amount of adsorbate removed from the liquid phase by unit mass of adsorbent at a constant temperature. Adsorption isotherms are basic requirements for the design of adsorption systems. The parameters of equilibrium isotherms often give useful information on sorption mechanism, surface properties and affinity of the adsorbent. It is therefore important to determine the most suitable correlation of equilibrium curves in order to optimize the conditions for designing adsorption systems [21]. In this study, the Langmuir, Freundlich and Temkin isotherms were tested to analyze the equilibrium data and the results as shown in (Table 1).

3.9. Langmuir Isotherm

Langmuir isotherm is used to describe adsorption phenomena and is based on the assumption that uptake occurs on a homogenous surface by monolayer sorption without interaction between adsorbed molecules. The linear form of the Langmuir isotherm equation [22] can be expressed in equation (6).

$$\frac{C_e}{q_e} = \frac{1}{q_L K_L} + \frac{C_o}{q_L} \dots\dots\dots (6)$$

where q_e is the monolayer adsorption capacity of the adsorbent (mg/g), K_L is the Langmuir adsorption constant (L/mg) related to the energy of adsorption which quantitatively reflects the affinity between the adsorbent and adsorbate and q_L is the maximum monolayer adsorption capacity of adsorbent (mg/g). The constants q_L and K_L can be determined from the slope and the intercept of the plot of $\frac{C_e}{q_e}$ against C_e .

The equilibrium biosorption data of Zn (II) ions for UPPAC, PPAC and CAC fitted reasonably well to the Langmuir isotherm. The Langmuir constant obtained for all the three adsorbents are summarized in (table 1). It can be seen that the correlation factor R^2 is close to the unity for Langmuir model, indicating a good representation of the experimental results by this model. The essential features of the Langmuir isotherm can be expressed in terms of a dimensionless constant

separation factor (R_L), defined by the relationship [23].

$$R_L = \frac{1}{1 + K_L C_o} \dots\dots\dots (7)$$

where C_o is the initial metal ion concentration in (mg/L) and K_L is the Langmuir equilibrium constant (L/mg). The value of the separation factor provides important information about the nature of the adsorption process. The adsorption is said to be irreversible ($R_L=0$), favorable ($0 < R_L < 1$), linear ($R_L=1$) or unfavorable if ($R_L > 1$). For the initial metal concentration from 200-1000 mg/L used in this study, the values of R_L ranged from 0.09-0.33; which indicates a favorable adsorption of Zn (II) ions onto UPPAC, PPAC, and CAC

3.10. Freundlich Isotherm

The Freundlich isotherm model assumes that the removal of metal ions occurs on a heterogeneous adsorbent surface and can be applied to multilayer adsorption [24]. The linear form of this isotherm equation is given as described in equation (8).

$$\log q_e = \log K_F + \left[\frac{1}{n} \right] \log C_e \dots\dots\dots (8)$$

where K_F (mg/g)(L/mg)^{1/n} and n are Freundlich adsorption constants related to the adsorption capacity and intensity of the adsorbents respectively. The constants were determined by the linear plot of $\log q_e$ versus $\log C_e$. These plots of $\log q_e$ versus $\log C_e$ for Zn (II) ions adsorption onto UPPAC, PPAC and CAC at 28°C were found to be linear. The magnitude of K_F and n show the ease of separation of heavy metal ions from metal contaminated water with high adsorption capacity. Table 1 shows the Freundlich adsorption isotherm constant and the correlation coefficients (R^2) obtained at 28°C. The magnitude of n gives an indication of the favorability of adsorption. It is generally stated that the values of n in the range 2-10 represent good, and less than 1, poor adsorption characteristic [25]. The isotherms were found to be linear as evidenced from correlation coefficients obtained in the range of 0.960 to 0.985. The Freundlich isotherm showed a better fit adsorption data than Langmuir isotherm suggesting heterogeneous nature of the adsorbents.

The value of K_F signifies adsorption intensity and higher K_F value of the three adsorbents confirmed the high adsorption capacity for Zn^{2+} . The higher value of K_F indicates higher affinity for metal ions and the values of n lie between 1 and 10 indicating favourable adsorption. This is in agreement with the finding of [26, 27].

3.11. Temkin Isotherm

The Temkin isotherm model unlike the Langmuir and Freundlich isotherms takes into account the interactions between adsorbents and metal ions to be adsorbed and is based on the assumption that the free energy of sorption is a function of the surface coverage [28]. The linear form of the Temkin isotherm model is expressed in equation (9).

$$q_e = B \ln A + B \ln C_e \dots\dots\dots (9)$$

where $B = RT/b_T$, T is the temperature (K), R is the ideal gas

constant (8.314 J/molK) and A is the equilibrium binding constant (L/mg) corresponding to the maximum binding energy. The plots of q_e versus $\ln C_e$ for the metal ions adsorbed onto UPPAC, PPAC and CAC at 28°C were found to be linear. The plot of q_e versus $\ln C_e$ enables the determination of A and B. The values of regression coefficient (R^2) for Zn (II) ions are lower than that of the Freundlich and Langmuir isotherm model. Therefore the adsorption of Zn (II) ions onto UPPAC, PPAC and CAC does not fit the Temkin as well as the Freundlich isotherm does.

Table 1. Comparison of the Langmuir, Freudlich and Temkin isotherm constants for the adsorption of Zn (II) onto UPPAC, PPAC and CAC.

Isotherm model	Adsorbents		
	UPPAC	PPAC	CAC
Langmuir			
q_L (mg/g)	342.7	351.4	358.3
K_L (L/mg)	0.0074	0.0093	0.0114
R^2	0.973	0.960	0.958
Freundlich			
K_F (mg/g)(mg/L) ^{1/n}	20.61	30.06	38.11
N	2.57	2.94	3.22
R^2	0.977	0.975	0.96
Temkin			
A (L/g)	0.106	0.229	0.301
B (mg/g)	56.93	48.85	51.07
R^2	0.945	0.915	0.890

3.12. Kinetic Studies

Adsorption kinetic models were applied to the experimental data in order to analyze the rate of adsorption and possible adsorption mechanism of Zn (II) ions unto UPPAC, PPAC and CAC. The kinetic models applied in this study are the Lagergren pseudo-first-order, pseudo-second-order, intraparticle-diffusion equation and Elovich model.

3.13. Pseudo-First-Order

Lagergren proposed a pseudo first-order kinetic model. This model was successfully applied to describe the kinetics of many adsorption systems [29]. The integral form of the model equation is expressed in equation (10).

$$\log(q_e - q_t) = \log q_e - \frac{k_1}{2.303} t \dots \dots \dots (10)$$

where, q_e and q_t (mg/g) are the amount of Zn (II) that was adsorbed at the equilibrium and at time t (min), respectively and k_1 (1/min) is the rate constant. The calculated values of the rate constant, k_1 , q_e and the corresponding coefficient, R^2 were calculated from the slopes and intercepts of $\log(q_e - q_t)$ against the t plots and were presented in the (table 2). The pseudo first order plot of Zn (II) adsorption on UPPAC, PPAC and CAC is shown in (figure 12). The lower correlation coefficients obtained suggest that the adsorption of Zn (II) on prepared activated carbons does not follow the pseudo first order kinetics.

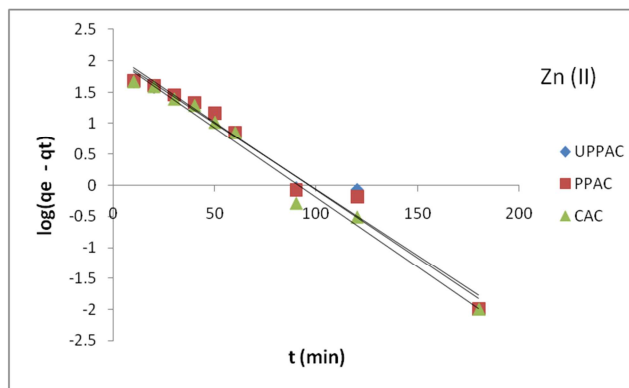


Fig. 12. Pseudo-first-order plots for adsorption of Zn (II) on UPPAC, PPAC and CAC.

3.14. Pseudo-Second-Order

The adsorption kinetics may also be described by a pseudo-second-order kinetics model [30]. The linearised integral form of the model is represented as

$$\frac{t}{q_t} = \frac{1}{k_2 q_e^2} + \frac{t}{q_e} \dots \dots \dots (11)$$

$$\text{and } h = k_2 q_e^2 \dots \dots \dots (12)$$

Where q_e and q_t (mg/g) are the amount of Zn (II) that was adsorbed at the equilibrium and at time t (min) respectively, k_2 is the pseudo-second-order rate constant of adsorption (g/mg min) and h is the initial adsorption rate at time t approaching 0 (mg/g min). This model has been widely used to evaluate adsorption rates [31]. This model is based on the assumption that chemisorption is the rate determining step [32].

From the slopes and intercepts of the linear plots obtained by plotting $\frac{t}{q_t}$ versus t , the values of the pseudo-second-order rate constants q_e and k_2 were calculated and given in (table 2). The pseudo second order plots of Zn (II) adsorbed on UPPAC, PPAC and CAC is shown in (figure 13). For all three types of adsorbents used, the results showed a very good compliance with the pseudo-second-order equation with high regression coefficients. The regression (R^2) values obtained are very close to unity and the adequate fitting of the plots confirmed that the adsorption of Zn (II) by the UPPAC, PPAC, and CAC followed pseudo-second-order kinetics. The result is in agreement with the finding of [33]. Also the theoretical (calculated) values of q_e for pseudo-second-order reaction model are closer to the experimental value of q_e as shown in (table 2). It could be observed then that for the entire sorption period, pseudo-second-order expression better predicts the sorption kinetics than the pseudo-first-order model. This suggests the assumption behind the pseudo-second-order model that the metal uptake process is due to chemisorptions [34]. Chemical sorption can occur by the polar functional groups of lignin, which include alcohols, aldehydes, ketones, acids, phenolic hydroxides and ethers as chemical bonding agents [35]. The values of h follow the trend CAC>PPAC>UPPAC indicating that CAC adsorbs Zn (II) more rapidly than PPAC and UPPAC.

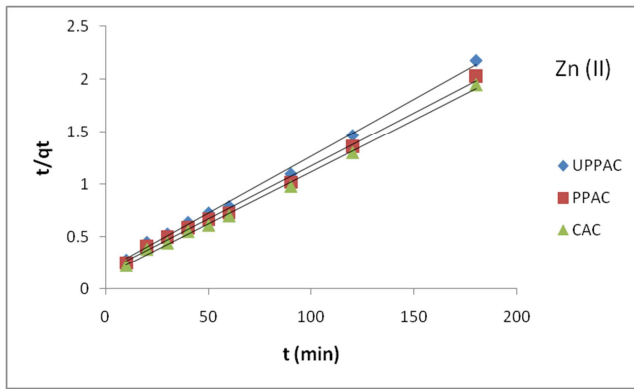


Fig. 13. Pseudo-second-order plots for adsorption of Zn (II) on UPPAC, PPAC, CAC.

3.15. Intra-Particle Diffusion

Weber and Morris model is widely used to predict the rate controlling step [36] in intra-particle diffusion model. When mass transfer is the controlling step, it is important to identify the diffusion mechanism. According to intra-particle diffusion model, the initial rate of diffusion is given by equation (13).

$$q_t = k_d t^{1/2} + I \dots\dots\dots (13)$$

where k_d is the intra-particle diffusion rate constant ($\text{mg/gmin}^{1/2}$) and I is the intercept. The intercept of the plot indicated the boundary layer effect. The larger the intercept, the greater the contribution of the surface sorption in the rate controlling step. The constant k_d was obtained from the slope of the plot of q_t versus $t^{1/2}$. Intra-particle diffusion is the sole rate-determining step if the plot is linear and passes through the origin. From (figure 14), it shows the plots did not pass through the origin but was close to it. This deviation from the origin is due to the difference in the rate of mass transfer in the initial and final stages of the adsorption process [37]. Moreover, the presence of the boundary layer effect (I) showed the existence of the surface sorption indicating that intra-particle diffusion was not the only rate-limiting step.

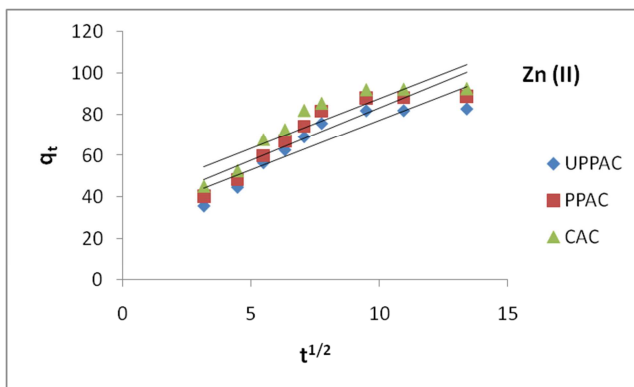


Fig. 14. Intra-particle diffusion plots for adsorption of Zn (II) on UPPAC, PPAC and CAC.

3.16. Elovich Equation

The Elovich equation has been applied by many scientists

in description of the kinetics of metal ion adsorption onto different adsorbents [38]. The linear form of the Elovich equation is given in equation (14).

$$q_t = \left(\frac{1}{\beta}\right) \ln(\alpha\beta) + \left(\frac{1}{\beta}\right) \ln t \dots\dots\dots (14)$$

where α is the initial adsorption rate (mg/g/min) and β is desorption rate constant (mg/g/min). Thus, a plot of q_t versus $\ln t$ yields a linear relationship with a slope of $\left(\frac{1}{\beta}\right)$ and an intercept of $\left(\frac{1}{\beta}\right) \ln(\alpha\beta)$ if the sorption process fits the Elovich equation. This equation was applied by a linear plot of q_t versus $\ln t$, illustrated in (Fig 15). The constants α and β were calculated from the intercept and slope of the plot of q_t versus $\ln t$ and presented in (Table 2). The values of α show that CAC had the highest initial adsorption rate. The value of R shown in (Table 2) varied between 0.913 and 0.939. This shows that the Elovich model did not give the best fit for the sorption process.

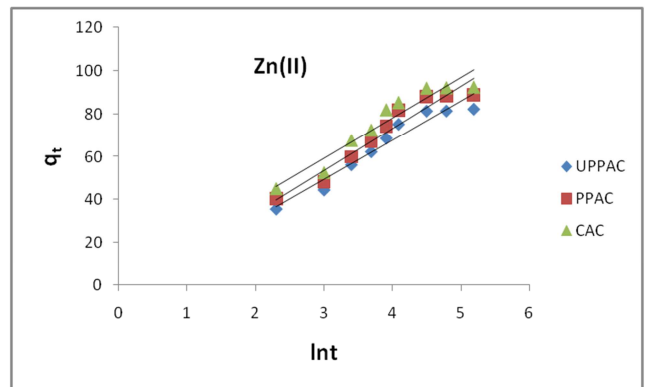


Fig. 15. Elovich plot for adsorption of Zn (II) on UPPAC, PPAC and CAC.

Table 2. Kinetic parameters for Zn (II) using UPPAC, PPAC and CAC as adsorbents.

Kinetic models	Adsorbents		
	UPPAC	PPAC	CAC
Pseudo-first-order			
q_e (Calculated)(mg/g)	117.2	127.64	111.94
q_e (Experimental)	82.46	88.96	92.36
K_1 (min^{-1})	0.048	0.048	0.051
R^2	0.970	0.976	0.984
Pseudo-second-order			
q_e (Calculated)(mg/g)	100	100	111.1
q_e (Experimental)	82.46	88.96	92.36
K_2 (g/mgmin)	0.000543	0.000606	0.000614
h_o	5.43	6.06	7.58
R^2	0.996	0.995	0.996
Intraparticle-diffusion			
I	4.775	5.101	4.840
k_d ($\text{mg/gmin}^{1/2}$)	29.29	32.14	39.07
R^2	0.826	0.830	0.799
Elovich equation			
α (mg/gmin)	13.50	15.21	22.21
β (g/min)	0.0545	0.0513	0.0534
R^2	0.939	0.936	0.922

3.17. Thermodynamic Study

The values of ΔH° and ΔS° were calculated from the slope and intercept of the plot ($\ln K_C$ versus $1/T$) shown in (figure 16). The free energy change (ΔG°) indicates the degree of spontaneity of the adsorption process and higher negative value reflects a more energetically favorable adsorption. The increase in negative value of ΔG° with increase in temperature shows that adsorption of Zn (II) on UPPAC, PPAC and CAC increased with rise in temperature. The ranges of ΔG° values for zinc ion are from -1.269 to -3.941 KJ/mol for UPPAC, -1.684 to -4.660 KJ/mol for PPAC and -1.952 to -5.530 KJ/mol for CAC. ΔG° was higher in CAC, showing that CAC was able to remove Zn (II) more than the other adsorbents.

The values of ΔH° obtained for the metal ions are positive indicating endothermic nature of the adsorption process, which explains the fact that adsorption efficiency increased with increase in temperature. Generally, the physical adsorption is exothermic and chemical adsorption is endothermic, so it was inferred that the chemisorptions took part in the adsorption process. The calculated enthalpy (ΔH°) values of UPPAC, PPAC and CAC for Zn^{2+} were 18.00 KJ/mol, 20.46 KJ/mol and 23.45 KJ/mol respectively.

The positive value of ΔS° indicated an increase in

randomness at the solid/liquid interface during the sorption process. The values of entropy changes (ΔS°) of Zn (II) were found to be 63.50 J/mol/K, 72.77 J/mol/K and 83.47 J/mol/K for UPPAC, PPAC and CAC as shown in (table 2). The result followed the order CAC>PPAC>UPPAC. Based on thermodynamics, negative ΔG° value and positive ΔH° and ΔS° values give a spontaneous process at high temperatures. Other workers [39, 40 & 41] have also reported similar results.

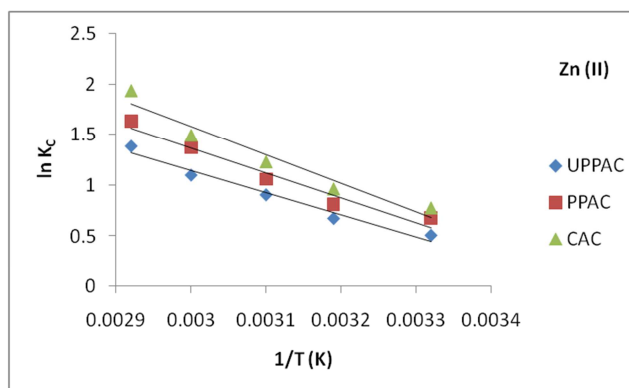


Fig. 16. Plot of $\ln K_C$ vs. $1/T$ for adsorption of Zn (II) on UPPAC, PPAC and CAC samples: initial metal concentration 400 mg/L, pH 6 and contact time 120 minutes.

Table 3. Thermodynamic parameters for the adsorption of Zn (II) by UPPAC, PPAC and CAC.

Adsorbent	T(K)	K_C	ΔG° (KJ/mo)	ΔH° (KJ/mo)	ΔS° (KJ/mol)
UPPAC	301	1.661	-1.269	18.00	63.50
	313	1.959	-1.749		
	323	2.470	-2.428		
	333	2.996	-3.037		
	343	3.981	-3.941		
PPAC	301	1.961	-1.684	20.46	72.77
	313	2.247	-2.108		
	323	2.876	-2.748		
	333	3.920	-3.782		
	343	5.126	-4.660		
CAC	301	2.182	-1.952	23.45	83.47
	313	2.630	-2.516		
	323	3.430	-3.311		
	333	4.464	-4.142		
	343	6.952	-5.530		

4. Conclusions

In this work, biosorption of Zn^{2+} on unripe plantain peel activated carbon, pineapple peel activated carbon, and commercial activated carbon was investigated in batch mode. The percent adsorption (% R) were determined to be a function of solution pH, contact time, adsorbent dose, initial concentration of heavy metal ions and temperature.

The SEM analysis of CAC, PPAC and UPPAC shows that they are very porous and that they have cavities for the adsorption of Zn (II) ions. The FTIR spectra of CAC, PPAC and UPPAC show that several peaks were observed in the spectra which indicated that they are composed of various functional groups which are responsible for the binding of the cations. The percentage removal (% R) increased with increase in pH,

contact time, temperature and adsorbent dose. The results obtained showed that CAC>PPAC>UPPAC for Zn^{2+} .

The linear regression of the experimental results for Zn^{2+} fitted better to the Freundlich than the Langmuir and Temkin model isotherms. This suggests that the biosorption system of CAC, PPAC and UPPAC could have more than one functional group which is responsible for the metal binding. The higher R^2 values (>0.99) for second-order parameters for the entire sorption period confirms that the sorption follows a pseudo-second-order mechanism. The pseudo-second-order expression better predicted the sorption kinetics of the metal ion adsorption onto CAC, PPAC and UPPAC than pseudo-first-order and intra-particle model. Thermodynamic constants were also evaluated using equilibrium constants at different temperatures. The positive values of ΔH° and ΔS° and negative value ΔG° indicates the endothermic and

spontaneous nature of the adsorption process.

The successful application of pineapple peel activated carbon and unripe plantain peel activated carbon as biosorbent introduces a less expensive environmentally friendly method for removal of metal ions from aqueous solution.

Acknowledgements

We are grateful to the department of chemistry, department of chemical engineering and soil science department in Federal University of Technology, Owerri, Imo state, Nigeria.

References

- [1] Taha, S., Ricordel, S., Cisse, I., and Dorange, G. (2001). "Heavy metals removal by adsorption onto peanut husk carbon: characterization, kinetic study and modeling", *Separation and Purification Technology*, Vol. 24, 389-401.
- [2] Guo, J., Qi, S., Yang, K., Yu, Z. and Wang, H. (2002). "Rice husk as a potentially low cost biosorbent for heavy metal and dye removal: an overview", *Materials Chemistry and Physics*, Vol. 78, pp. 132-137.
- [3] Fenglian, F., and Wang Q. (2011). Removal of heavy metal ions from wastewater, *Journal of Environmental Management*, 92, 407-418.
- [4] USDHHS (1993). *Toxicological profile for zinc*, US Department of Health and Human Services, Agency for Toxic Substances and Disease Registry, Atlanta Georgia.
- [5] Walsh, T., Sandstead, H. T., Prasad, A. S., Newberne, P. M., and Fraker, P. J. (1994). "Zinc: health effects and research priorities for the 1990s", *Environmental Health Perspectives*, vol. 102, pp. 5-46.
- [6] Khan, M. N., Wahab, M. F., (2006). Characterization of chemically modified corncobs and its application in the removal of metal ions from aqueous solution. *J. Hazard Mater.* B 141, pp 237-244.
- [7] Namasivayam, C., and Ranganathan, K. (1995). Removal of Pb (II), Cd (II), Ni (II) and Mixture of Metals ions by Adsorption onto 'Waste' Fe (III)/Cr (III) hydroxide and fixed bed studies. *Environ. Technol.* 16, 851 – 860.
- [8] Kannan, N., and Rengasamy, G. (2005). Comparison of cadmium ion adsorption on various activated carbons, *Water Air Soil Pollut.* 163, 185-201.
- [9] Alvarez-Ayuso, E. Garcia-Sanchez, A. and Querol, X. (2003). Purification of metal electroplating waste waters using zeolites, *Water Research*, 37, 4855-4862.
- [10] Uzoiye A., Uche, C. C., and Ashiegbu, D. (2013). Analysis of Thermodynamics, kinetics and equilibrium isotherm on Fe³⁺/Fe²⁺ adsorption onto palm kernel shell activated carbon (PKSAC): A low-Cost adsorbent. *American Chemical Science journal (ACSJ)*.
- [11] Tan, W. T., Ooi, S. T., and Lee, C. K. (1993). Removal of Chromium (VI) from solution by coconut husk and palm pressed fibers. *Environmental Technology*, 14, 277-282.
- [12] Dwivedi, C. P., Sahu, J. N., Mohanty, C. R., Raj Mohan, B., and Maikap, B.C. (2008). Column performance of granular activated carbon packed bed for Pb (II) removal. *Journal of Hazardous Materials*, 156 (1-3), 596-603.
- [13] Liang, S., Guo, X., Feng, N., and Tian, Q. (2010). Isotherms, kinetics and thermodynamic studies of adsorption of Cu²⁺ from aqueous solution by Mg²⁺/K⁺ orange peel adsorbents. *J Hazard Mater*; 174, 756-62.
- [14] Derylo-Marczewski, A. D, Blanchind, M, Marczewske, A. W, Swiatkoweri, A, and Tarasiuk, B. (2010). Adsorption selected herbicides from aqueous solution on activated carbon. *J. Them Anal calorim* 100, 785-794.
- [15] Joseph, Y. F, and Noursh, E.(2013). Performance, Kinetic and equilibrium in biosorption of anionic of saccharomyces cerevisiae as a low-cost biosorbent. *Turkish J Eng. Evn. Sci.* 37, 146-161.
- [16] Periasamy, K., and Namas, C. V. (1995). Removal of Ni (II) from aqueous solution and nickel industry wastewater using an agricultural waste: peanut hull, *waste manage.* 15, 54-63.
- [17] Shukla, A., Zhang, Y. H., Dubey, P., Margrave, J. L., and Shukla, S. S. (2002). The role of sawdust in the removal of unwanted material from water, *J. Hazard. Mater*; B95, 137-152.
- [18] Tsia, W. T., and Chen, H. R. (2010). Removal of malachite green from aqueous solution using low-cost charcoal based biomass. *J. Hazard. Mater*; 175, 844-849.
- [19] Hamadaoni, O., and Chiha, M. (2007). Removal of methylene blue from synthetic wastewater by wheat bran, *Acta chim. Slov.* 54, 407-418.
- [20] Meena, A. K., Mishra, G. K., Rai, P. K., Rajagopal, C., & Nagar, P. N. (2008) Removal of heavy metal ions from aqueous solutions using carbon aerogel as an adsorbent. *Journal of Hazardous Materials*, 150, 604-611.
- [21] Vaghetti, J. C. P., Lima, E. C., Rogers, B., Brasil, J. L., Dacunha, B. M., and Simon, N. M. (2008). Application of Brazilian-Pine fruit coat as biosorbent for removal of Cr (IV) from aqueous solution: kinetic and equilibrium study. *Biochem Eng. J.* 42, 67-76.
- [22] Allen, S. J., Mckay, G., and Porter, J. F. (2004). Adsorption isotherm models for basic dye adsorption by peat in single and binary component systems. *Journal of Colloid Interface Science*, 280, 322 – 333.
- [23] Anirudan, T. S., and Radhakrishnan P. G. (2008). Thermodynamic and kinetics of adsorption of Cu (II) from aqueous solution onto a new cation exchanger derived from tamarind fruit shell. *J. Chem Thermodyn*, 40, 702-709.
- [24] Adamson, A. W., and Gast, A. P. (1997). *Physical Chemistry of Surfaces*, sixth ed. Wiley-Interscience, New-York.
- [25] Aksu, Z., and Kutsal, T. (1991). A biosorption process for removing lead (II) ions from wastewater by using *C. vulgaris*. *Journal of Chemical Technology and Biotechnology*, 52, 109-118.
- [26] Brown, P. A., Gill, S. A., and Allen, S. J. (2000). Metal removal from wastewater using peat. *Water Res.*, 34, 3907-3916.
- [27] Lakatos, J., Brown, S. D., and Snape, C. E. (2002). Coals as sorbent for the removal and reduction of hexavalent chromium from aqueous waste streams. *Fuel*, 81, 691-698.

- [28] Chen, Z., Ma, W., and Han, M. (2008). Biosorption of nickel and copper onto treated alga (*undariapinnarlifida*): application of isotherm and kinetic models. *J Hazard Mater*: 155, 327-333.
- [29] Bhattacharyya, K. G., and Sharma, A. (2005). Kinetics and thermodynamics of methylene blue adsorption on Neem (*Azadirachta indica*), *Dyes Pigments* 65, 51-59
- [30] Ho, Y. S. (2006). Second-order kinetic model for the biosorption of cadmium onto tree fern: a comparison of linear and non-linear methods. *Water Research*, 40, 119-125.
- [31] Ho, Y. S., and McKay, G. (2000). The kinetics of biosorption of divalent metal ions onto sphagnum moss peat. *Water research*; 34, 735-742.
- [32] Ho, Y. S., and McKay, G. (1998). Biosorption of dye from aqueous solution by peat. *Chemical Engineering Journal*, 70, 115-124.
- [33] Kumar, K. V. and Porkordi, K. (2007). Mass transfer, kinetics and equilibrium studies for the biosorption of methylene blue using *Paspalum notatum*. *J. Hazard mater*, 146, 214-226.
- [34] Ho, Y. S and McKay, G. (2003). Removal of copper ions from aqueous solution by tree fern. *Water Res*, 37, 2323-2330.
- [35] Vadivelan, V. and Kumar, K. V. (2005). Equilibrium, kinetics, mechanism and process design for the sorption of methylene blue onto rice husk. *Journal of colloid and interface science*, 286, 90-100.
- [36] Mane, V. S., Mall, I. D., and Srivastava, V. C. (2007). Use of bagasse fly ash as an adsorbent for the removal of brilliant green dye from aqueous solution, *Dyes Pigments*. 73, 269-278.
- [37] Das, B., and Mondal, N. K. (2011). Calcerous soil as a new adsorbent to remove lead from aqueous solution: equilibrium, kinetic and thermodynamic study. *Univ. J. environ Res Technol*; 1 (4): 515-530.
- [38] Juang, R. S. and Chen, M. L. (1997). 'Application of the Elovich Equation to the Kinetics of Metal Sorption with Solvent Impregnated Resins', *Ind Eng. Chem Res*. 36, 813-820.
- [39] Dawodu, F. A. Akpomie, G. K., and Ejikeme, P. C. N. (2012). Equilibrium, Thermodynamic and Kinetic Studies on the Adsorption of lead (II) from Solution by "Agbani Clay". *Research Journal of Engineering Sciences*, Vol. 1(6), 9-17.
- [40] Li, P. J., Ke, X., Zhou, Q. X., Zhang, Y. and Sun, T. H. (2006). Removal of heavy metals from a contaminated soil using tartaric acid. *Journal of Environmental Science, China*. 18, 727-733.
- [41] Prabakaran, R., and Arivoli, S. (2012). Adsorption kinetics, equilibrium and thermodynamic studies of Nickel adsorption onto *Thespesia populnea* bark as biosorbent from aqueous solutions. *European journal of Applied Engineering and Scientific Research*. 1 (4), 134-142.